ISSN 2070-2051, Protection of Metals and Physical Chemistry of Surfaces, 2009, Vol. 45, No. 1, pp. 46–53. © Pleiades Publishing, Ltd., 2009.

MOLECULAR AND SUPRAMOLECULAR STRUCTURES AT THE INTERFACES

Inhibition Effects of Methionine and Tyrosine on Corrosion of Iron in HCl Solution: Electrochemical, FTIR, and Quantum-Chemical Study[1]

S. Zor, F. Kandemirli, and M. Bingul

Department of Chemistry, Kocaeli University, Kocaeli, 41380, Turkey

Received October 26, 2007

Abstract—The inhibiting effect of methionine and tyrosine on the corrosion of iron is researched electrochemically in 0.1M HCl, Quantum chemical calculations were performed. The level of HF with the 6–311G(d,p) basis set for methionine and tyrosine. Corrosion current density has been determined by polarization measures and the inhibition effect was calculated. With an increase in the concentration of inhibitor, the effectiveness of inhibition increases. The highest inhibition is determined as 97.8% at 100 ppm methionine. The effect of temperature is determined by chronoammetric measures. Surface analysis is performed with FTIR spectroscopy. Methionine and tyrosine adsorb on the iron surface according to Langmiur isotherm. The highest occupied and the lowest unoccupied molecular orbital energy, as well as Mulliken and atomic charges with hydrogens summed into heavy atoms of C, N, O, S atoms and of methionine, tyrosine, and protonated forms have been examined.

PACS numbers: 81.65.Kn, 68.43.-h

DOI: 10.1134/S2070205109010079

INTRODUCTION

Acidic solutions are used in many industrial areas. The most important application are acid pickling, industrial acid cleaning, acid descaling, and oil well acidising [1, 2]. Various methods are investigated to protect the metals from corrosion in acidic solutions. The studies of inhibitive effect of organic molecules are progressive. Organic molecules rich in heteroatoms as oxygen, sulfide and nitrogen provide the best protection from metal corrosion [3–13]. Various organic compounds used as inhibitors in industrial applications blockade the metal surface by adsorbing on the metal surface physically and chemically. Adsorbed inhibitors prevent the occurrence of cathodic or anodic reactions or both of them.

The adsorption effect of inhibitive molecules depends on the structure of a molecule, corrosion environment, the charge and nature of metal surface, and the interaction type between metal surface and organic molecule [7–11].

In recent studies, the search on compounds such as azol, aminoacids, aminoesters, and pyridine, containing nitrogen and sulfur, are in progress [7–15]. Oguzie et al. found methionine functions as an inhibitor of mild steel corrosion in 0.5 M H_2SO_4 solution. A mixed-inhibiting mechanism is proposed for the protective effect increased with concentration [16]. On the other hand, quantum chemical studies have been successfully performed to link the corrosion inhibition efficiency with molecular structure levels for some kinds of organic compounds, e.g. imidazole [17], amides [18, 19], etc.

The aim of the present study was to examine inhibitive action of the afore mentioned inhibitors toward the corrosion of iron in HCl solution and to investigate structure and inhibitor relationship.

EXPERIMENTAL

Hydrocloric acid (HCl, Merch, 35–37%) methionine, and tyrosine (Sigma Aldrich) were used as received. Armco iron was used for the electrochemical measurements. Iron electrode was armored in polyester, with a surface area of 0.785 cm^2 in contact with the corrosive media. The electrode was first polished successively with metallographic emery paper up to 600 grits. The electrode was then washed with distilled water, degreased with acetone, washed using distilled water again, and then inserted immediately into the glass cell containing 250 ml of the electrolyte solution.

Polarization experiments were carried out in a conventional three-electrode electrochemical cell. Pt electrode was the counter one, Saturated Calomel Electrode (SCE) was as the reference one, and iron electrode was the working. Polarization curves were recorded by changing the electrode potential from –250 to +250 mV

[1] The text was submitted by the authors in English.

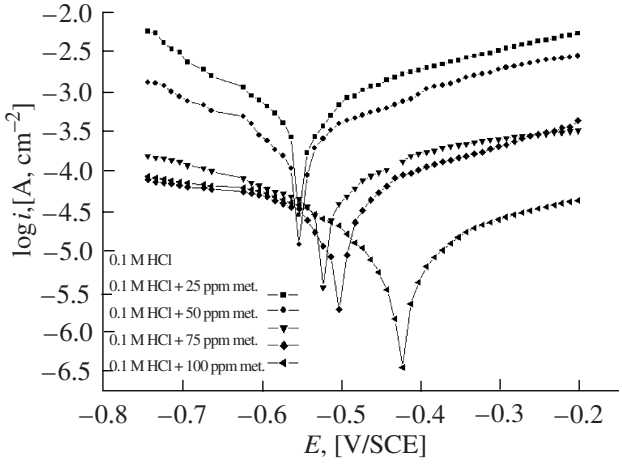

Fig. 1. Polarization curves of iron with and without methionine in 0.1M HCl.

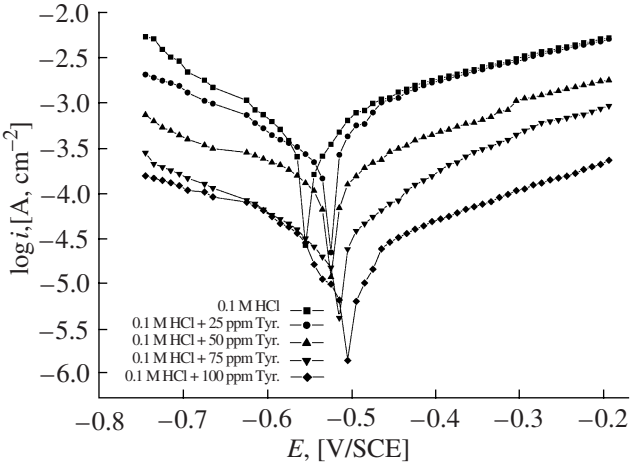

Fig. 2. Polarization curves of iron with and without tyrosine in 0.1 M HCl.

(SCE) with scan 10 mV/s using potentiostate-galvanostate (EG 8 PAR model 263).

Potentiostatic experiments were performed to test the current response to different inhibitor injections. Corrosion current density (i_{corr}) before and after adding inhibitor as determined using the Tafel extrapolation method.

The inhibiting efficiency, IE (%) is calculated from potentiodynamic data by the formulae:

$$\mathrm{IE} = \frac{(i_{corr})_o - (i_{corr})_{inh}}{(i_{corr})_o} \times 100.$$

Where $(i_{corr})_o$ and $(i_{corr})_{inh}$ are the uninhibited and inhibited corrosion current densities respectively, determined by extrapolation of Tafel lines.

Chronoammetric measurements were carried on at a constant potential. At different temperatures of inhibitors current–time curves were obtained.

FTIR Analysis. For the FTIR analysis, iron plates were dipped for 10 days in solutions with and without inhibitor. The FTIR spectra (400–4000 cm^{-1}) have been recorded on using a Shimadzu 8201/86601 PC spectrometer The spectrum of the protective film formed on the surface was recorded using FTIR after drying, mixing it with KBr, and making a pellet out of it.

Quantum Chemistry Analysis. The molecule sketch of methionine and tyrosine was drawn in the Gauss View and the quantum calculations were performed using Gaussian 03 (Revision B.05) [20] software. The relationship between inhibition efficiency of methionine and tyrosine and its electronic property were carried out at the level of HF with the 6–311G(d,p) basis set.

RESULTS AND DISCUSSION

Polarization Measurements

Polarization curves in solutions including or not [including methionine and tyrosine and in different concentrations (25, 50, 75, 100 ppm)] are given in Figs. 1 and 2, respectively. In both polarization curves, methionine and tyrosine decrease anodic and cathodic current density, compared with and without inhibitor. Accordingly, the inhibitor molecules show mixed inhi-

Table 1. Electrochemical corrosion parameters for iron in 0.1M HCl with and without inhibitor

Conc.	Icorr ($\mu A/cm^2$)	-Ecorr (mV)	Rp	E, %
0.1 M HCl	187	556	108	
25 ppm met.	98.7	556	398	47.2
50 ppm met.	20.9	525	4463	88.8
75 ppm met.	10.3	506	12195	94.5
100 ppm met.	4.23	426	21875	97.7
25 ppm tyr.	147	526	162	21.4
50 ppm tyr.	76	526	1485	59.3
75 ppm tyr.	45.3	515	6320	75.7
100 ppm tyr.	20.3	506	10596	89. 1

bition mechanism, counteracting both cathodic and anodic reactions and hence reforming acidic solutions.

Electrochemical parameters i_{corr} (corrosion current density) Rp (polarization resistance), E_{corr}(Corrosion potential) obtained from polarization curves, are given in Table 1.

One sees that with an increase in the concentration of inhibitor the effect of inhibition increases. Although both methionine and tryrosine is effective, the greatest effect is observed in 0.1M HCl solutions containing 100 ppm methionine. The inhibition efficiency reaches its best with methionine (E = 97.7%), which has a sulphur atom in the molecule; the presence of free electron pairs in this atoms plays the major part in the adsorption. Corrosion potential particularly changes toward more positive values in solutions containing methionine. Polarization resistance increases in solutions.

It is generally accepted that the first step in the adsorption of an organic inhibitor on a metal surface usually involves the replacement of water molecules adsorbed at the metal surface [15];

$$Inh_{(sol)} + XH_2O_{(ads)} \longleftrightarrow Inh_{(ads)} + XH_2O_{(sol)}.$$

The second step is occurrence of metal–inhibitor complexes with freshly generated Fe^{2+} ions on the steel surface.

$$Fe \longrightarrow Fe^{+2} + 2e^-,$$

$$Fe^{+2} + Inh_{(ad)} \longrightarrow Fe(Inh)^{+2}ads.$$

Thus it is possible to suggest that at low concentrations, the amount of inhibitor molecules in the solution is insufficient to form a compact complex with the metal ions. As the concentration is increased, more inhibitor molecules become available for complex formation [7].

The inhibition process is based on the adsorption of the amino acid molecules at the active sites and/or deposition of corrosion products on the metal surface [13, 14]. So an increase in the efficiency of inhibition with the inhibitor concentration indicates that more its molecules are adsorbed on the metal surface, thus leading to a greater surface coverage.

Besides, amino acids are protonated in acidic solutions [9].

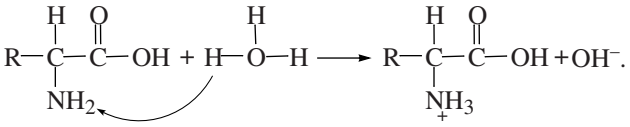

It is generally accepted that the presence of halide ions in acidic media synergistically increases the inhibition efficiency of some organic compounds [7]. In halide-containing acidic solutions, especially chloride ions, are considered as pit initiators [21], the metal surface is mostly covered with adsorbed layer of the halide ions, the amino acid molecule with its protonated form will be adsorbed on the active sites, where the Cl^- are already present according to the following formulation [13]:

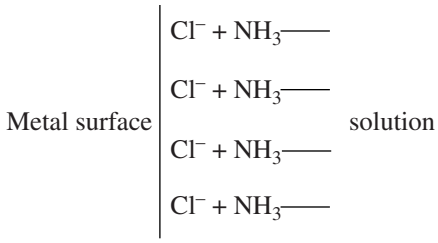

i.e. the adsorption of the amino acid is enhanced in the presence of the halide ions [13, 22].

It is thought that the halide ions are able to improve adsorption of the organic cations by forming intermediate bridges between the positively charged metal surface and organic inhibitor [7]. The inhibition effectiveness largely depends on the amount of adsorbed chloride ions on active Fe sites of the electrode.

In acidic solution methionine can be protonated at the amine group, even though the presence of $S–CH_3$ decreases the stability of the positive charge. The inhibitor could interact with the corroding steel surface via the protonated amino function, which can be adsorbed at cathodic sites and hinder the hydrogen evolution reaction or via the S atom in the aliphatic chain, which may adsorb at anodic sites and retard Fe electrochemical dissolution. Thus was observed a mixed inhibition mechanism [7, 11]. Electron in aromatic ring of the tyrosine can be shared with iron orbitals, thus forming insoluble complex that protect the surface from aggressive ions.

In the inhibition with tyrosine, only protonated amine group is effective. But in the methionine, sulfide atom which is inside the aliphatic chain, is also effective besides protonated amine group. For this reason, methionine is more effective than tyrosine (Table 1).

Chronoammetric Measurements. Chronoammetric curves of iron containing 25 and 100 ppm methionine and tyrosine in 0.1M HCl at different temperatures (298, 308, 323, 343 K) are given in Figs. 3 and 4.

In all the chronoammetric curves, current values have not changed in time at constant temperatures. However, with an increase in temperature, the current values have increased. In solvents with 25 ppm methionine, the current values at 298 K have increased by 25% at 308 K; by 57% at 323 K; and 64.7%, at 343 K (Fig. 3a). In solvents with 100 ppm methionine, the increase in the currents were 21% at 208 K, 45% inat 323 K, and 50% at 343 K (Fig. 3b).

With 25 ppm tyrosine, the increase was 40%, 56%, and 66% respectively when compared to 298 K. In 100 ppm tyrosine, this ratio was 25% (308 K), 45% (323 K), and 62.5% (343 K) (Figs. 4a and 4b).

According to chronoammetric results, with an increase in the inhibitor concentration, the effect of temperature decreases. Corrosion accelerates with an

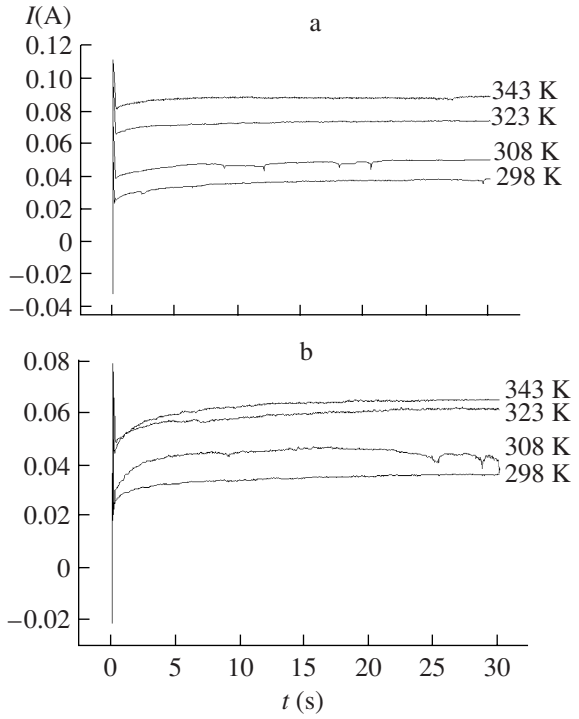

Fig. 3. Chronoammetric curves of iron at different temperatures in 0.1M HCl a) 25 ppm methionine, b) 100 ppm methionine.

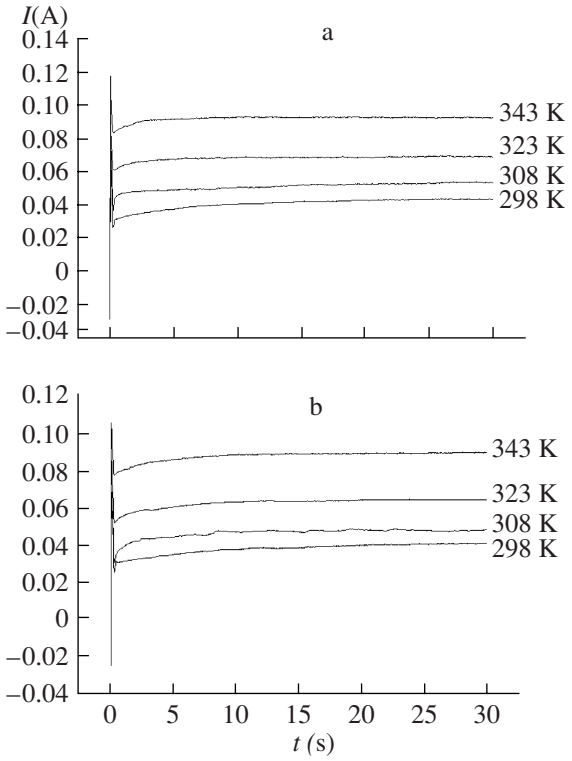

Fig. 4. Chronoammetric curves of iron in different temperatures in 0.1M HCl a) 25 ppm tyrosine, b) 100 ppm tyrosine.

increase in temperature, stimulating both anodic and cathodic reactions.

Adsorption Isotherm. To receive more information about interaction between the aminoacid molecules and the metal surface, various isotherms are tested. The Langmuir one obtained fits straight-line the best. This isotherm is used to explain the monolayer adsorption of inhibitor molecules. It can be written as follows:

$$\ln\frac{\theta}{1-\theta} = \ln c + \ln A - \frac{\Delta G}{RT},$$

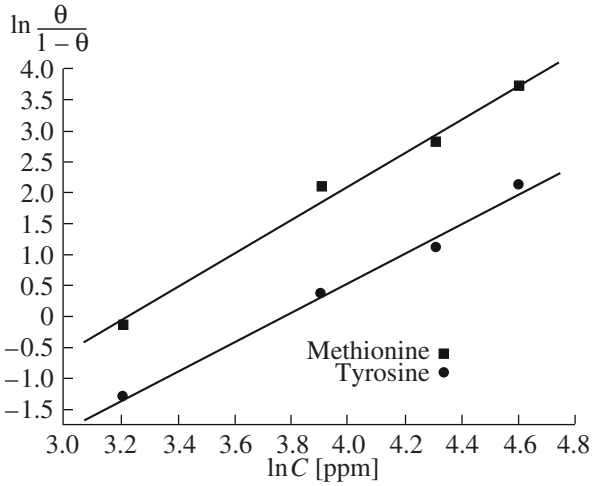

Fig. 5. Langmiur adsorption isotherm curves of iron in 0.1M HCl with methionine and tyrosine.

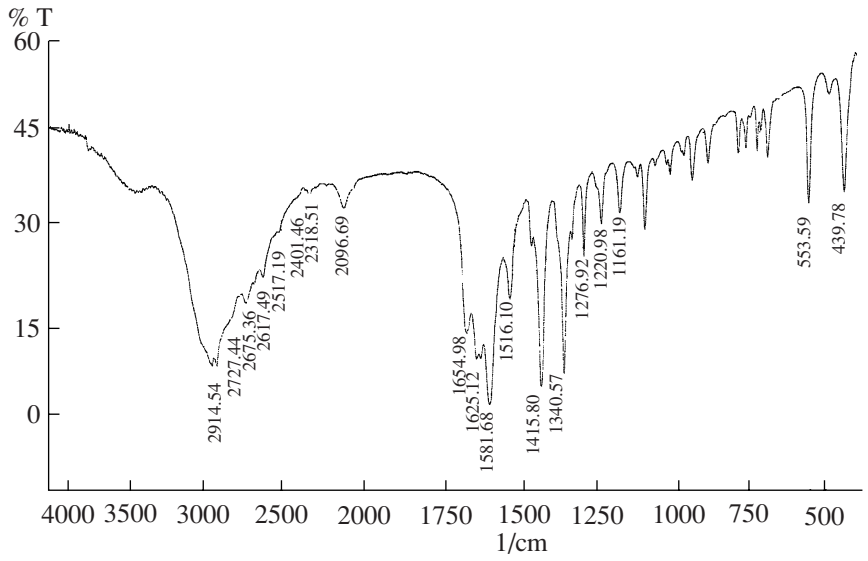

Fig. 6. FTIR spectrum of pure methionine.

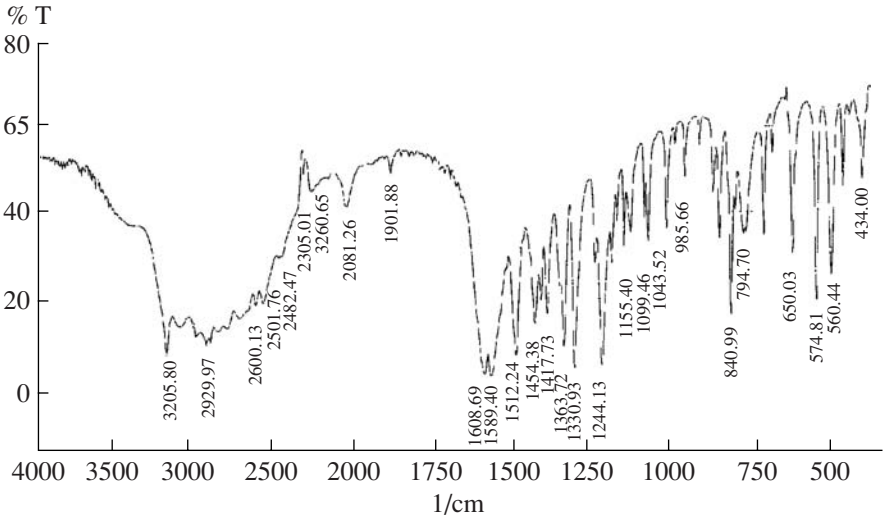

Fig. 7. FTIR spectrum of pure tyrosine.

$$\frac{\theta}{1-\theta} = K_c \exp\left(-\frac{\Delta G}{RT}\right),$$

where θ is the surface coverage area, K_c is the constant of adsorption, ΔG is the free energy of adsorption, and c is the inhibitor concentration. The fraction of surface covered by adsorbed molecules of inhibitor (θ) is expressed by the radio IE(%)/100 (Fig. 5).

The values of ΔG^0_{ads} are obtained, namely, –23.1 and –21.72 kJ/mol, for methionine and tyrosine, respectively. This kind of isotherm is generally regarded to indicate physical adsorption.

FTIR Results. The FTIR spectrum of pure methionine is given in Fig. 6. In the spectrum, a characteristic peak of methionine is seen. In 1660 cm^{-1}, C=O stretching, in 1620 and 1580 cm^{-1} N–H stretching, and in 1070 cm^{-1} C–N stretching is seen. Also, C–S–C stretching is 560 cm^{-1}. The FTIR spectrum of pure tyrosine is given in Fig. 7. In the spectrum, the aromatic C–H stretching is in 3040 cm^{-1} C–H out of plane curve is in 2000–1600 cm^{-1}. Aromatic C=C stretching is in 1580 cm^{-1}, –NH stretching is in 1512 cm^{-1}, C–N stretching- in 1330 cm^{-1}, N–H inner plane bending in 1043 cm^{-1} and 840 cm^{-1}, and C–H out of plane in 780–650 cm^{-1} (Fig. 6).

FTIR spectra of the film layer formed on iron surface upon 30 days in 0.1 M HCl, containing and not

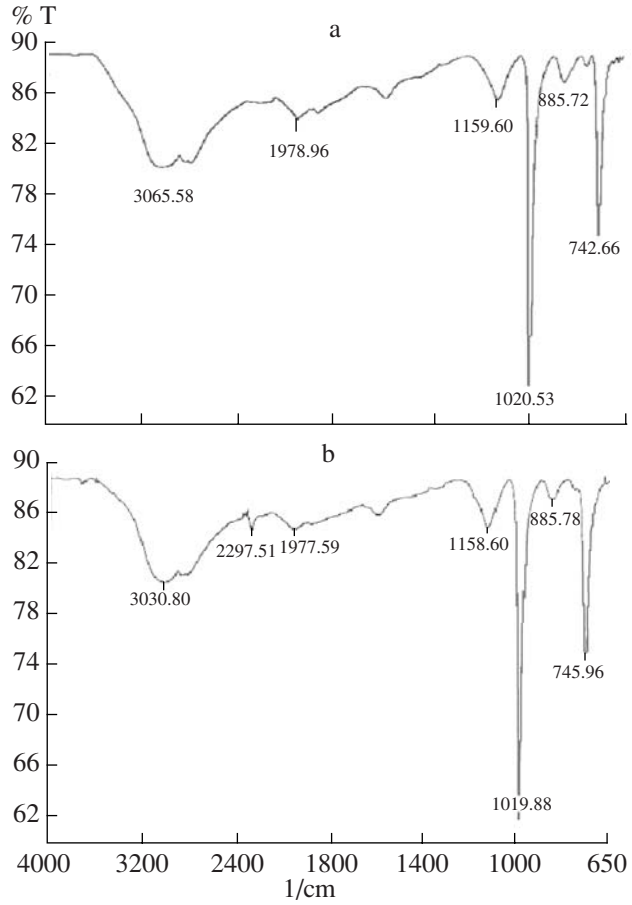

Fig. 8. FTIR spectrum of films formed on iron after immersion in 0.1M HCl a) 0.1M HCl, b)0.1M HCl + 100 ppm methionine.

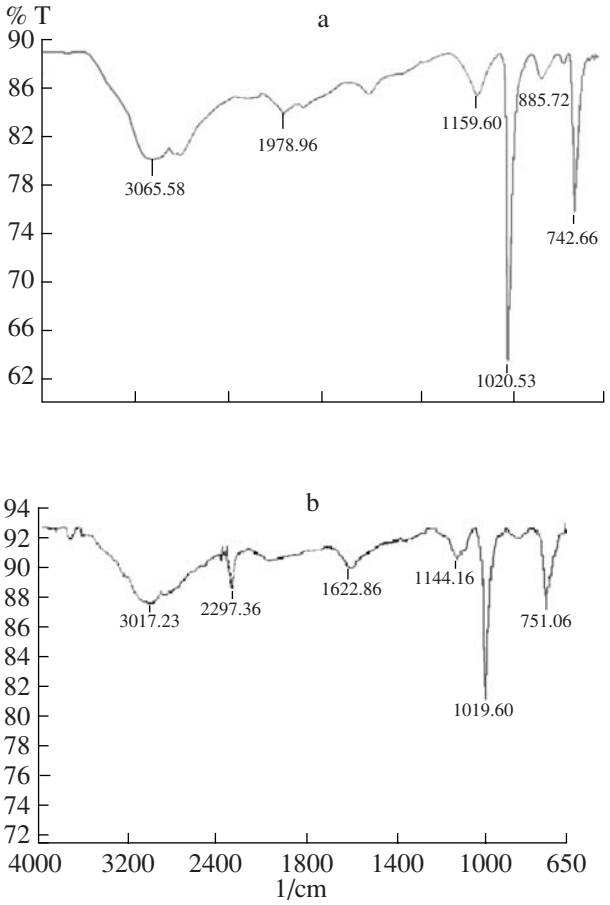

Fig. 9. FTIR spectrum of films formed on iron after immersion in 0.1M HCl a) 0.1M HCl, b)0.1M HCl + 100 ppm tyrosine.

100 ppm methionine and tyrosine, are given in Figs. 8 and 9 respectively. In both of them (a) is the curve of the film layer formed on metal surfaces without the inhibitor and (b) is a similar curve but formed with the inhibitor. Distinctive characteristic peaks in pure methionine and tyrosine spectra disappeared completely (compare Figs. 6, 7 and 8, 9). The spectrum curves with and without the inhibitor (a and b) are similar. In other words, peaks that correspond to each other in the same frequency are obtained (Figs. 8 and 9). According to this conclusion, methionine and tyrosine are adsorbed physically on the metal surface. ΔG values that are obtained from Langmuir adsorption isotherm also support this result.

Quantum Chemistry Calculations. The quantum chemistry calculation method was an advantaged measurement to screen out the effective inhibitors prior to other experiments. The optimum geometry of the methionine and tyrosine was shown in Fig. 10. Theoretical calculations predict 18 stable conformations of neutral tyrosine. For each of the three conformations of the amino acidic moiety, three different orientations of the phenol ring with respect to the amino group have been found. The theoretical calculations have revealed that the most stable form of tyrosine is one of the conformations and intermolecular hydrogen bond exists between the hydroxylic H atom and the lone pair of the amino N atom and phenyl ring pointed toward the amino group [23].

Figure 11 was the highest occupied molecular orbital (HOMO) population and the lowest unoccupied molecular orbital (LUMO) population of methionine and tyrosine. HOMO orbital was populated mainly around the sulphur atom for methionine. HOMO and LUMO orbitals for tyrosine consist of mainly phenyl ring.

Frontier orbitals play important role in chemical adsorption, but in acidic solution, methionine and tyrosine can be protonated at the amine group. Chloride ions (from HCl) have a small degree of hydration and bring excesses negative charges in the vicinity of the interface [24]. The protonated methionine and tyrosine might adsorb onto the metallic surface via the negatively charged chloride ions. The proceeding of physical adsorption requires the presence of electrically charged metal surface and charged species in the bulk

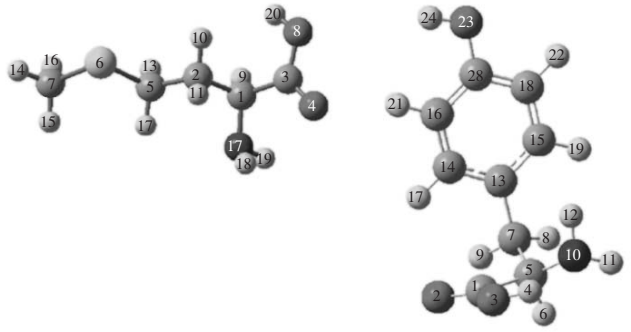

Methionine Tyrosine

Fig. 10. Optimized with HF/6–31G(d,p) molecular structures of methionine and tyrosine (ball and stick model).

of the solution [16]. Table 2 lists the bonds length and angles of methionine, tyrosine and protonated forms. The effect of the protonation weakens the C3–O8 and S6–C5 bonds slightly for methionine and O2–C1 and C1–C5 for tyrosine.

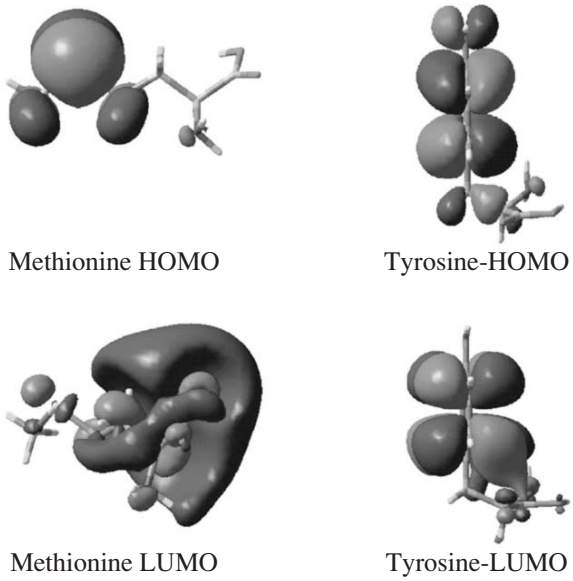

Methionine HOMO Tyrosine-HOMO

Methionine LUMO Tyrosine-LUMO

Fig. 11. Population of highest occupied molecular orbital (HOMO) and LUMO of methionine and tyrosine.

Table 2 lists the Mulliken charges and atomic charges with hydrogens summed into heavy atoms of C, N, O, S atoms and of methionine, tyrosine and pro-

Table 2. Values for atom distances (Å) and angles (degree) of methionine, tyrosine and protonated forms

Bond	Meth	$MethH^+$	Bond	Tyr	Tyr H^+
C7–S6	1.809	1.811	C5–N10	1.457	1.507
S6–C5	1.818	1.814	C1–C5	1.533	1.526
C5–C	1.525	1.531	O2–C1	1.181	1.170
C–C1	1.539	1.535	C7–C5	1.540	1.539
C1–N17	1.443	1.504	C13–C7	1.516	1.515
C1–C3	1.531	1.533	C14–C13	1.391	1.390
C3–O4	1.176	1.176	O23–C20	1.350	1.336
C3–O8	1.334	1.305	O3–C1	1.316	1.323
Angle			Angle		
C7-S6-C5	100.107	100.55	C1-C5-N10	109.9	109.68
S6-C5-C	110.02	108.62	O2-C1-C5	122.7	122.50
C-C1-N17	110.59	110.87	C7-C5-C10	116.0	110.34
C3-C1-N17	112.76	104.606	C13-C7-C5	114.8	113.68
H19-N17-C1	110.57	111.57	C14-C13-C7	121.5	121.56
H21-N17-C1	–	112.24	C15-C13-C7	120.9	121.14

Table 3. Charges of methionine, tyrosine and protonated forms

	Mulliken Charges		Atomic charges with hydrogens summed into heavy atoms	
Atoms	Meth	$MethH^+$	Meth	$MethH^+$
C7	–0.390	–0.396	–0.016	0.038
S6	0.051	0.116	0.051	0.116
C5	–0.292	–0.320	–0.023	–0.068
C2	–0.186	–0.201	0.049	0.122
C1	–0.121	–0.190	–0.003	0.004
N17	–0.462	–0.302	–0.062	0.623
C3	0.550	0.629	0.550	0.629
O4	–0.421	–0.411	–0.421	–0.411
08	–0.387	–0.340	–0.124	–0.053
Atoms	Tyr	Tyr H^+	Tyr	Tyr H^+
C1	0.591	0.591	0.613	0.613
O2	–0.457	–0.457	–0.385	–0.385
O3	–0.452	–0.112	–0.454	–0.126
C5	–0.083	0.056	–0.122	0.081
C7	–0.107	0.137	–0.132	0.216
C13	–0.179	–0.179	–0.227	0.179
N10	–0.560	–0.125	–0.306	0.607
O23	–0.453	–0.192	–0.426	–0.150

tonated forms. Mulliken charge of S atom goes from 0.051 electron (unprotonated) to 0.116 electron and N atom goes from –0.462 electron to –0.302 electron for methionine.

In Table 3 the atomic charges with hydrogens summed into heavy atoms are also shown. The atomic charges with hydrogens for C7 (0.038 ē), S6 (0.116 ē), C2 (0.122 ē), C3 (0.629 ē), N17 (0.623 ē) atoms are positive for protonated methionine. The atomic charges with hydrogens for C1 (0.613 ē), S6 (0.116 ē), C7 (0.216 ē), C5 (0.081 ē), and N10 (0. 0.607 ē) atoms are positive for protonated tyrosine. The atomic charges with hydrogens of nitrogen atom for protonated methionine are larger than those for protonated tyrosine. So, atomic charge of protonated amines play important role in adsorption.

CONCLUSIONS

1. Both methionine and tyrosine were effective in the inhibition of iron. But most effective was methionine.

2. As inhibitor concentration increased, the effect of inhibition also increased.

3. It is shown that with an increase in temperature, the current in chronoammetric curves also increases. Thus, the corrosion rate of iron accelerates.

4. The adsorption of methionine and tyrosine accords with Langmuir adsorption isotherm. The obtained spectrum curves and ΔG values, show that physical adsorption may be effective in adsorption of inhibitors on metal surface.

5. Quantum chemical calculations performed for methionine and tyrosine, as well as, their protonated structures, corroborate that both theoretical and experimental inhibition effect of methionine ion on Fe in HCl solution is better than that of tyrosine.

REFERENCES

1. Chebabe, D., Ait Chikh, Z., Hajjaji, N., et al., *Corros. Sci.*, 2003, vol. 45, p. 309.
2. Khaled, K.F. and Hackerman, N., *Matter. Chem. Phys.*, 2003, vol. 82, p. 949.
3. Zor, S., Yazici, B., and Erbil, M., *Corros. Science*, 2005, vol. 47, p. 2700.
4. Zor, S., Dogan, P., and Yazici, B., *Corros. Review,* 2005, vol. 23, p. 217.
5. Zor, S. and Dogan, P., *Corros. Rev.*, 2004, vol. 22, p. 209.
6. Zor, S. and Turk, *J. Chem.*, 2002, vol. 26, p. 403.
7. Oguzie, E.E., Li, Y., and Wang, F.H., *J. Colloid and Interface Sci.*, 2007, vol. 310, p. 90.
8. Elayyachy, M., Idrissi, A.El., and Hammouti, B., *Corros. Sci.*, 2006, vol. 48, p. 2470.
9. Yurt, A., Bereket, G., and Ogretir, C., *Theochem.*, 2005, vol. 725, p. 215.
10. Zerfaoui, M., Oudda, H., Hammouti, B., et al., *Progress in Organic Coatings,* 2004, vol. 51, p. 134.
11. Ashassi-Sorkhabi, H., Ghasemi, Z., and Seifzadeh, D., *Appl. Surface Sci.*, 2005, vol. 249, p. 408.
12. Silva, A.B., Agostinho, S.M.L., Barcia, O.E., et al., *Corros. Sci.*, (in press).
13. Badawy, W.A., Ismail, K.M., and Fathi, A.M., *Electrochem. Acta*, 2006, vol. 51, p. 4182.
14. Bereket, G. and Yurt, A., *Corros. Sci.*, 2001, vol. 43, p. 1179.
15. Bockris, J.O. and Swinkels, D.A.J., *J. Electrochem. Soc.,* 1964, vol. 11, p. 746.
16. Lebrini, M., Lagrene`e, M., Vezin, H., et al., *Corros. Sci.*, 2005, vol. 47, p. 491.
17. Fang, J. and Li, J., *Journal of Molecular Structure (Theochem)*, 2002, vol. 593, p. 179.
18. Kandemirli, F. and Sagdinc, S., *Corros. Sci.*, 2007, vol. 49, p. 2118.
19. Bereket, G., Ogretir, C., and Yurt, A., *Journal of Molecular Structure (Theochem)*, 2001, .vol. 571, p. 139.
20. Frisch, M.J., Trucks, G.W., Schlegel, H.B., et al., *Gaussian 03, Revision B.05*, Wallingford, CT: Gaussian, Inc, 2004.
21. Munoz, A.I., Anton, J.G., Guinon, J.L., and Herranz, V.P., *Elecrochem. Acta,* 2004, vol. 50, p. 957.
22. Badawy, W.A., Ismail, K.M., and Fathi A.M., *J. Appl. Electrochem.*, 2005, vol. 35, p. 879.
23. Ramaekers, R., Pajak, J., Rospenk, M., and Maes, G., *Spectrochem. Acta. Part A*, 2005, vol. 61, p. 1347.
24. Luo, H., Guan, Y.C., and Han, K.N., *Corrosion.*, 1998, vol. 54, p. 721.